A Model of Cortical Associative Memory Based on a Horizontal Network of Connected Columns

Erik Fransén and Anders Lansner*

SANS – Studies of Artificial Neural Systems
Dept. of Numerical Analysis and Computing Science
Royal Institute of Technology, S–10044 Stockholm, Sweden

*To whom correspondence should be addressed
Email: ala@sans.kth.se
FAX: +46-8-790 0930, TEL: +46-8-790 6210

(submitted)

Abstract

Attractor network models of cortical associative memory functions have developed considerably over the past few years. Here we show that we can improve them further, in terms of correspondence with cortical connectivity, by using multiple cells in lamina II/III of cortical columns connected by long-range fibers as the functional unit in the network instead of just a single cell. The connectivity of the model then becomes more realistic, since the original dense and symmetric connectivity now may be sparse and strongly asymmetric at the cell-to-cell level. Our simulations show that this kind of network, with model neurons of the Hodgkin-Huxley type arranged in columns, can operate as an associative memory in much the same way as previous models having a simpler connectivity. Cell activities comply with experimental findings and reaction times are within biological and psychological limits. By introducing a scaling model we make it plausible that a network approaching experimentally reported neuron numbers and synaptic distributions also could work like the studied network.

1 Introduction

1.1 Background

Studies on short-term *i.e.* (Fuster and Jervey 1982; Funahashi *et al.* 1989; Miyashita and Chang 1988) and long-term *i.e.* (Miyashita 1988) memory tasks have revealed elevated firing rates for cells in the prefrontal cortex during the memory demanding delay period of match-to-sample experiments. Much of this work is reviewed by Goldman-Rakic (1995). It is reported that *in vivo* experiments show that closely adjacent pyramidal and non-pyramidal neurons with similar preferences show opposite activity. When the one cell increases its firing rate the other decreases its rate (Wilson *et al.* 1994; Goldman-Rakic 1995). This is different from what is found in the primary visual cortex where suppression of activity is strongest for an optimal stimulus orientation (Douglas *et al.* 1991) (*i.e.* excitation and inhibition seem to work in the same direction). Further, in the review by Goldman-Rakic (1995) it is hypothesized that cells with the same preference are excitatorily connected both locally (within a column) and long-range, and that cells with opposite (or dissimilar) preference provide mutually inhibitory action on each other. This mutual inhibition between differently coding columns has not been shown in visual cortex where connections between iso-orientation columns seem to dominate.

The elevated rates and opposed excitatory and inhibitory activity pattern of prefrontal neurons is consistent with what is produced in a recurrent attractor artificial neural network (ANN). An auto-associative memory based on an attractor network produces elevated activity for the cells in the retrieved memory. If the learning rule that produced the connectivity is of a correlation based (Hebbian) type, cells active in the same memory can get connected by excitatory synapses and cells active in different memories get inhibitorily connected. In our columnar network this makes nearby excitatory and inhibitory cells display opposite activity changes.

Attractor network models of cortical associative memory functions *i.e.* (Hopfield 1982; Smolensky 1986; Lansner and Ekeberg 1989; Amit *et al.* 1990) display several features that may be described in Gestalt psychological terms. When a partial pattern is presented, the full pattern is retrieved. If two patterns are presented simultaneously, a rivalry process leads to a competition between the patterns where one pattern may defeat the other. The attractor networks have developed considerably over the past few years. During the development they have also been criticized on several points, *i.e.* low storage capacity, slow convergence time and high firing rates, but computer simulations done by ourselves and others have refuted most of this criticism (Lansner and Fransén 1992; Fransén *et al.* 1993; Fransén and Lansner 1995b). Additionally, structural support for these ideas based on distributed processing comes from *e.g.* Goldman-Rakic (1988) and Cavada and Goldman-Rakic (1989). In that work the authors use the term "multiple

nodal links". These links connect regions by multiple and usually reciprocal connections. A remaining drawback, however, of the ANN models has been their lack of a biologically reasonable connectivity in that they are usually based on an all-to-all and symmetric connectivity between neurons. The real cortical connectivity pattern is much more complex, extremely sparse (at least in general) and is also likely to be mainly asymmetric. It also shows considerable locality in that most connections are between nearby cells, and long connections get progressively more infrequent.

In the work presented here, the functional units from the ANN are assumed to be represented by lamina II/III cells in cortical columns instead of single cells as in our previous model (Lansner and Fransén 1992). Preliminary results of this columnar based model have been presented previously (Lansner and Fransén 1995). The cells in each column correspond to a single unit in an ANN. This makes the connectivity from the ANN model look more like that of real cortex, since it becomes sparse, especially for the long-range connections, and also asymmetric at the level of single cells. The aim of this work is to show that such a network can operate as an associative memory in much the same way as an attractor ANN, and as our previous model using realistic neurons and synapses with a simple connectivity (Lansner and Fransén 1992; Fransén and Lansner 1995a). By introducing a set of scaling equations we also want to make it plausible that a network approaching experimentally reported neuron numbers and synaptic distributions also could work like the studied network.

Our column model includes only the lamina II/III pyramidal cells and inhibitory interneurons, and the afference from lamina IV. It thus corresponds primarily to the horizontal network connecting cells in the different columns, and the local network within lamina II/III. From experimental observations the pyramidal cells are said to be dominated by input from lateral connections, and not by afference (Martin 1988). Further, most horizontal connections go between lamina II/III pyramidal cells (Gilbert and Kelly 1975; McGuire *et al.* 1991). This lamina is also especially thick in the frontal and parieto-temporal "association" areas (Rockel *et al.* 1980). The activity of lamina IV, the major afference (Gilbert and Wiesel 1979; Kisvarday *et al.* 1989; Ferster and Lindström 1985; Blasdel *et al.* 1985), is here modeled by the stimulation supplied to the neurons. In the model several simplifications have obviously been done. For instance: other afference, the minor direct thalamocortical input (Ferster and Lindström 1983) as well as the small input (excitatory and inhibitory) from lamina V and VI (Kisvarday *et al.* 1989; Ferster and Lindström 1983; Somogyi *et al.* 1983; Blasdel *et al.* 1985) have been omitted. For the associative memory function studied here they are assumed to merely play a modulatory role. Further, there is only one type of interneuron included and there is no inhibition on these.

A modular description of cortex has been put forward by *i.e.* Mountcastle (1957), Hubel and Wiesel (1962), and Szentágothai (1978). Anatomic evidence for a patchy structure has been obtained by for instance a combi-

nation of 2-deoxyglucose autoradiography and retrograde labeling (Gilbert *et al.* 1990; McGuire *et al.* 1991). A functionally patchy structure has been shown *in vivo* by cross-correlation analysis (Hata *et al.* 1993; Ts'o *et al.* 1986) and *in vitro* by a multi-site stimulation technique combined with whole-cell patch clamp for recording (Weliky and Katz 1994). Weliky and Katz report strong correlations between nearby cells, which is consistent with our column model where several cells have similar afference and recruit each other in order to operate as one functional unit. The view of a patchy (columnar) structure of the neocortex has support not only in primary sensory areas (orientation columns, ocular dominance columns, color blobs, vibrissa barrels) but is also found in association areas *i.e.* entorhinal cortex (Hevner 1993) as discussed by Hevner and Wong-Riley (1992).

1.2 Outline of the model

In this study we have used the general purpose simulators, SWIM and SPLIT, intended for numerical simulation of networks of biologically realistic model neurons (Ekeberg *et al.* 1994, 1991; Hammarlund and Ekeberg 1996). Details of the mathematical model of cells and synaptic transmission is found in (Ekeberg *et al.* 1991; Brodin *et al.* 1991; Wallén *et al.* 1992; Tråvén *et al.* 1993; Fransén and Lansner 1995b).

The cells used in the simulations described here are of intermediate complexity. They are of the regularly spiking pyramidal cell type (RS) with 6 compartments, or the non-adapting fast spiking inhibitory type (FS) with 3 compartments. Voltage dependent ion channels for Na, K, Ca, and Ca-dependent K are modeled using Hodgkin-Huxley-like equations. There are two calcium pools, one with a faster time constant (Ca-channel related) and one with a slower time constant (NMDA-channel related). The excitatory RS-RS glutamate synapse is of a mixed kainate/α-amino-3-hydroxy-5-methyl-4-isoxazolepropionic acid (AMPA) and N-methyl-D-aspartate (NMDA) type. The RS-FS synapse has only a fast kainate/AMPA component. The inhibitory FS-RS synapse is of the fast $GABA_A$ type.

The network consists of 750 cells in 50 columns. Each column is composed of 12 pyramidal cells and 3 fast spiking inhibitory interneurons, see fig. 1 and fig. 2 (left). Within a column the pyramidal cells connect to each other densely. The inhibitory interneurons only contact the local pyramidal cells. The excitatory long-range (inter-columnar) connectivity is from pyramidal cells in the sending column to pyramidal cells in the receiving column. Inhibitory drive is from pyramidal cells in the sending column to the inhibitory interneurons in the receiving column. Thus local connectivity is dense and both excitatory and inhibitory, whereas the long-range (inter-columnar) connectivity is sparse and exclusively excitatory. Further, although the functional (effective) connectivity between columns is all-to-all and symmetric, the cell-to-cell connectivity is strongly asymmetric and sparse. The connectivity which determines the long-range synaptic efficacy

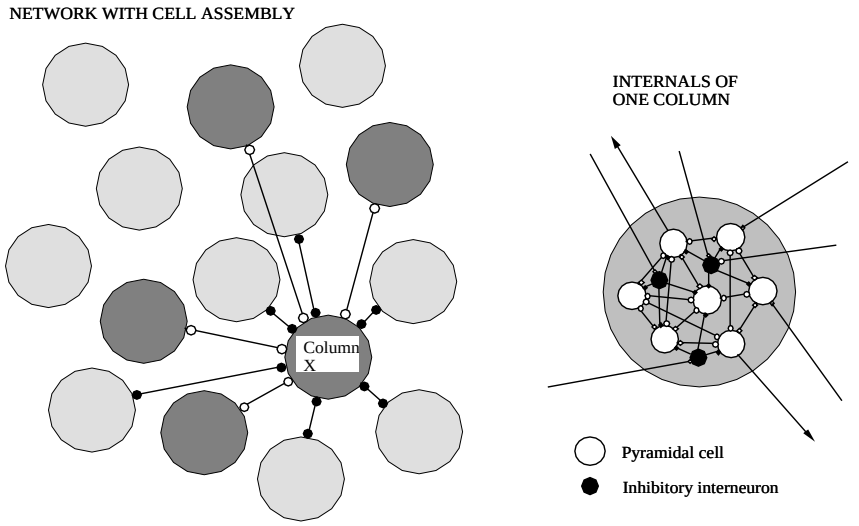

Figure 1: Left: Part of the model network shown for comparison with the corresponding attractor ANN. Each filled circle is a column/network unit. Darker columns are in the same cell assembly. The connectivity of "Column X" is shown. Each intracolumnar connection shown represents multiple synaptic connections. Right: Internal structure of one column comprised of excitatory pyramidal cells (white) and local inhibitory interneurons (dark). Incoming excitatory connections make contact directly onto pyramidal cells whereas inhibition is disynaptic as seen from a pyramidal cell.

---

was created using an ANN and then incorporated into our network model. The memories that are recalled in the present simulations are the assemblies/patterns that have been stored in the artificial neural network by the learning rule of the ANN. The model will be described in detail in the next three sections.

2 Structure of the Network Model

The basic network consists of 50 columns connected by horizontal long-range connections. Larger examples will be discussed in the section on scaling, 6. The connections between the columns were created using an ANN and then incorporated into our network model. Eight different assemblies/patterns, each composed of 8 out of 50 units/columns active, were stored in the network by a Bayesian correlation based (Hebbian) learning rule (Lansner and Ekeberg 1989; Lansner and Holst 1996), see appendix A. This gave in total 1960 excitatory synapses and 7392 inhibitory synapses. Patterns are overlapping, *i.e.* sharing some common columns. Connections get excitatory between columns that occur together in one or more of the stored patterns,

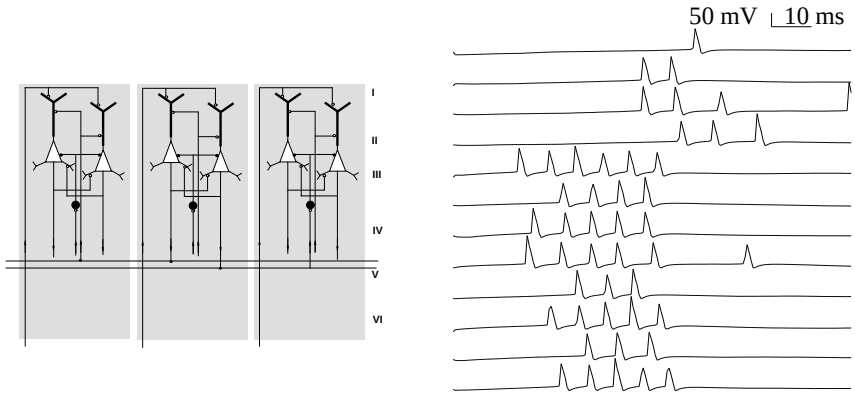

Figure 2: Left: Wiring diagram (lateral view) for the network model simulated. Three columns are shown, the two leftmost ones belong to the same assembly. Right: Completion within one column. Soma membrane potential of all 12 pyramidal cells in one column for a simulation of 100 ms and modulator application 60%. The lower 8 of the pyramidal cells were stimulated with 0.2 nA for 50 ms and the remaining 4 were indirectly activated.

and inhibitory between those columns that never occur together in any of the patterns. This is consistent with a hypothesis of prefrontal cortex which proposes that cells with the same preference are excitatorily connected and cells with opposite (or dissimilar) preference provide mutually inhibitory action on each other (Goldman-Rakic 1995). Further, in prefrontal cortex it has been shown that closely adjacent pyramidal and nonpyramidal neurons show opposite activity. When the one cell increases its firing rate the other decreases its rate (Goldman-Rakic 1995). This kind of activity also appears in our network as will be shown in sect. 5.3.

Each column is composed of 12 pyramidal cells and 3 fast spiking inhibitory interneurons. This gives the 80% excitatory and 20% inhibitory neurons reported by Gilbert *et al.* (1990) and Katz and Callaway (1992) and represents a sub-sampling in terms of cell numbers. Within a column the pyramidal cells connect to each other at the basal dendrite by a total of 70 randomly chosen synapses. A basal placement of local excitatory synapses is described by Nicoll and Blakemore (1993). The latency of the connection is 1.2 ms as found by Mason *et al.* (1991) with a standard deviation of 2.5%. Within the column our inhibitory interneurons each make a contact to the soma of 8 pyramidal cells. Thus every pyramidal cell receives input from two inhibitory cells. The latency is the same as for the RS-RS connection. In cortex, a lamina II/III basket cell usually connects to pyramidal cells in its own column (Martin 1988). The basket cell connects on the soma or proximal dendrites of the pyramidal cell (Nicoll 1994; Buhl *et al.* 1994). A pyramidal cell is contacted by several (10) basket cells and every basket cell contacts many (300) pyramids (Martin 1988).

In the model, many long-range connections (one per presynaptic cell) converge on the apical dendrite of the RS-cell. Apical placement of long-range excitatory synapses is reported by Gilbert *et al.* (1990). A very sparse (presumed singular) connectivity on vertically oriented dendrites (presumed apical) has been found (McGuire *et al.* 1991). Here, the RS-RS excitatory long-range connectivity between two columns is from 2 presynaptic pyramidal cells in the sending column to 6 postsynaptic pyramidal cells in the receiving column. Long-range connections on the inhibitory cells go from 6 presynaptic pyramidal cells in the sending column to the soma of the 3 inhibitory interneurons in the receiving column. This will give the fast rise time of the EPSP as reported for the corresponding synapses (Thomson and Deuchars 1994), due to a proximal or somatic placement. Each model pyramidal cell has one connection on the inhibitory interneuron as found by Buhl *et al.* (1994), and several cooperating inputs are needed to fire a cell (Somogyi and Martin 1985).

The modeled columns were placed on a rectangular grid with 1 mm separation representing a 7×7 mm patch of cortex. The long-range connections have a latency which varies with the "distance" between columns. With an axonal conduction velocity of 1 m/s (corresponding to unmyelinated intracortical fibers) the latency was 2.2–11 ms with an average of 5.0 ms. With myelinated fibers the distance between the columns can be much larger and still yield a latency of the same order of magnitude. A standard deviation of 2.5% was used when calculating each delay.

Thus, in the model the local connectivity is dense and both excitatory and inhibitory, whereas the long-range (inter-columnar) connectivity is sparse and exclusively excitatory. Further, although the functional (effective) connectivity between columns is all-to-all and symmetric, the cell-to-cell connectivity is strongly asymmetric and sparse. Partial support for recurrent (all-to-all) connectivity comes from the observation that long-range connections between areas are reciprocal and to multiple columns (Rockel *et al.* 1980; Gilbert *et al.* 1990). Also reciprocal connections between multiply interconnected regions are reported (Goldman-Rakic 1988; Cavada and Goldman-Rakic 1989). Further, in V1 symmetric columnar interactions may be present as exclusively iso-orientation columns are connected (Gilbert *et al.* 1990; Ts'o *et al.* 1986). A symmetric scheme may also be a result of the hypothesis by Goldman-Rakic (1995) as mentioned previously.

In section 6 a few resulting numbers (totals and proportions) are compared to experimental findings and related to scaling issues and model extensions.

3 The Cell and Synapse Models

3.1 The Neocortical Pyramidal Cell Model

Our model of the neocortical pyramidal cell of lamina II/III (Fransén and Lansner 1995b), RS, is based on the excitatory regularly spiking type cell (McCormick *et al.* 1985; Connors and Gutnick 1990). A short stimulation gives a relatively wide spike followed by an early and a late afterhyperpolarization (AHP) separated by a small depolarizing afterpotential. At longer stimulations the cell has a pronounced adaptation. The cell is modeled with 6 compartments (soma, initial segment, basal compartment and 3 serial apical compartments). The soma diameter is sampled from a normal distribution with a mean of $21\mu m$ and a standard deviation of 5 %. The dendritic tree has one apical and one basal branch separating synaptic input of different origin. Parameter values used here are found in the appendix C and were discussed previously (Fransén and Lansner 1995b).

3.2 The Fast Spiking Inhibitory Neuron

For the fast spiking inhibitory interneuron, FS (McCormick *et al.* 1985; Connors and Gutnick 1990), much less data is available. Essentially it is a non-adapting, fast spiking small cell with a small dendritic tree. It has been suggested that the inhibitory cell connecting to the lamina II/III pyramids belongs to the histologically defined basket cell type (Goldman-Rakic 1995; Martin 1988; McGuire *et al.* 1991; Kawaguchi 1995). The action potential repolarization of the modeled FS-cell is fast as reported by several investigators (McCormick *et al.* 1985; Connors and Gutnick 1990; Baranyi *et al.* 1993; Foehring *et al.* 1991) and the half amplitude width is 0.3 ms (McCormick *et al.* 1985; Baranyi *et al.* 1993). It has a large fast AHP as commonly found (McCormick *et al.* 1985; Connors and Gutnick 1990; Baranyi *et al.* 1993; Foehring *et al.* 1991; Kawaguchi 1995) with a depth of about 10 mV and half amplitude width of 8.0 ms, but virtually no slow AHP (McCormick *et al.* 1985; Connors and Gutnick 1990; Baranyi *et al.* 1993; Foehring *et al.* 1991). The cell is modeled with 3 compartments (soma, initial segment and dendrite). The soma diameter is sampled from a normal distribution with a mean of $7\mu m$ (McCormick *et al.* 1985; Foehring *et al.* 1991) and a standard deviation of 5 %. The membrane time constant is 8.7 ms as described by Kawaguchi (1995), which is in between the 7.2 (Baranyi *et al.* 1993) and 11.9 ms (McCormick *et al.* 1985) that was found in other work. The cell has a rather linear I-f curve up to some 200 Hz, and the primary I-f slope is much steeper than for the RS-cell (McCormick *et al.* 1985; Foehring *et al.* 1991). Parameter values and further discussions of them are found in the appendix C.

3.3 The Model Synapses

The model synapses used here are described by Brodin *et al.* (1991) and Tråvén *et al.* (1993). The excitatory RS-RS glutamate synapse is of a mixed kainate/AMPA and NMDA type with equally large peak amplitude postsynaptic potentials (PSP) for each type alone. In our simulations the NMDA conductance has been scaled up a factor of 7 compared to the AMPA conductance to get this relationship. Experimentally both the local (columnar) excitatory connections and the long-range connections are reported to have mixed responses (Thomson and Deuchars 1994). The model RS-FS synapse has only a fast kainate/AMPA component as reported by Thomson and Deuchars (1994). The inhibitory FS-RS synapse is assumed to be of the $GABA_A$ type as found experimentally (Thomson and Deuchars 1994). This is also consistent with reports that stimulation originating remotely, *e.g.* not in the home column, gives an essentially pure $GABA_A$ response (Hirsch and Gilbert 1991; Kawaguchi 1995). The model synapses are saturating corresponding to a full saturation of the postsynaptic receptor pool by one presynaptic activation (Fransén and Lansner 1995b). With these saturating synapses the spike rates are relatively low also when an assembly is fully active (Fransén and Lansner 1995b, 1995a). All synaptic conductances were sampled from a normal distribution with a standard deviation of 20%. The local RS-RS synaptic conductance is 0.38 nS and gives an soma EPSP of 0.81 mV. In experiments the EPSP amplitude of nearby cells has been reported to have a large variation with an average of 0.55 mV (Mason *et al.* 1991). Several active local inputs have been estimated to be necessary to activate a RS-cell (Nicoll and Blakemore 1993), which is also true for our model. Our long-range RS-RS synaptic conductance is on the average 1.4 nS which gives an EPSP of 2.5 mV. In cortex the synaptic strength of the long-range connections has been estimated to be one order of magnitude weaker than the local (Gilbert *et al.* 1990). Here the small number of afferent synapses (3.3 per cell) gives an artificially high value, see however the discussion in sect. 6. The model's long-range RS-FS synaptic conductance is on the average 0.072 nS which gives an EPSP of 2.2 mV. Experimentally, the pyramid to inhibitory interneuron strength has been reported to be variable with a mean of 0.66 mV in the range 0.31–0.92 mV (Buhl *et al.* 1994). Our local inhibitory synaptic conductance is 10.0 nS and gives an IPSP of 5.4 mV. In cortex the inhibition on a RS-cell from one basket cell is meditated by some 8–10 synapses (Martin 1988) and is relatively effective (Thomson and Deuchars 1994).

4 Background Activity and Input to the Network

In vivo recordings reveal that some cells have a higher background activity than others. This is commonly named background noise. Intracellular

recordings also show that resting potentials differ. We hypothesize that this might have a functional origin. One could interpret this as a way to control a cell's general firing likelihood. For the same synaptic efficacy a cell held close to the threshold is easily activated and a cell far from its threshold requires more input (higher frequency and/or more fibers active) to fire. If the synaptic efficacies are tuned by the Bayesian correlation based learning rule used here (Lansner and Ekeberg 1989) and appendix A, cells that take part in many patterns and hence are less discriminative and weaker indicators for any particular pattern, can get connected by weaker synapses. At the same time they get a higher bias (lower threshold) which allows the cell to be active despite the small synaptic strengths. In our network we have implemented the bias that decreases the threshold as a constant current injection. *In vivo*, the bias could come from for instance auto-regulated leakage channels. Having a bias in the presence of noise would make cells with a smaller threshold more active. Without direct input, the à *priori* probability of firing should be higher for a cell that is part of many patterns than for a cell that is part of just a few.

The simple model of the input from lamina IV to a column is a 50 ms current injection on 8 out of 12 RS-cells. To avoid common-input synchronization artifacts, current stimulation start and stop times were generated from a normal distribution with a standard deviation of 5 ms for each cell. All currents strengths were generated with a standard deviation of 10%. The stimulation of a pattern of columns has two components, see appendix A. If the columns belong to the stimulated pattern they are given a depolarizing current injection. If they are not part of the pattern they are given a hyperpolarizing current injection. This is a way to tell the network what is known to be present and not present. No stimulation would correspond to a "don't know" case, and the cell stays at its à *priori* firing frequency. The depolarizing component could in cortex come from the lamina IV granule cells. The hyperpolarizing component could be supplied by the lamina IV feed forward inhibitory cells (Martin 1988; Kisvarday *et al.* 1989; Somogyi *et al.* 1983). Depolarizing and hyperpolarizing currents are consistent with the finding in V1 that stimulation of the thalamo-cortical projection has been shown to give a monosynaptic excitation and disynaptic inhibition in lamina III (Gilbert *et al.* 1990; Hirsch and Gilbert 1991; Ferster and Lindström 1983).

5 Simulation Results

Here we will first demonstrate that a column is capable of acting as a functional unit. We will then show that an assembly of columns can give afteractivity and pattern completion, and thereafter show that competition between assemblies is operating properly. The qualitative behavior of these assembly operations is similar to that produced by a recurrent ANN (Lansner and Ekeberg 1989). The assembly operations have previously been shown

to work for a smaller network of connected pairs with one pyramidal cell and one fast spiking cell (Lansner and Fransén 1992).

The simulations were made on a SUN SPARCstation 5 and an IBM SP2 system both running UNIX. A time step of $50\mu s$ was used and a simulation of 500 ms took about 3 minutes of computing time on 4 SP2 Thin-II (RS/6000) nodes.

5.1 One Column

Our studies show that a single column can act as one functional unit analogous to an ANN-unit (Fransén and Lansner 1995b). As an example, if 8 of the 12 pyramidal cells in the same column are stimulated they can activate their non-stimulated companions in some 20–40 ms (fig. 2 right). If 4 cells are stimulated the completion is slower and weaker. If 2 cells are stimulated (which can be regarded as spurious activity) very little completion takes place, *i.e.* the column shows noise tolerance. No after-activity has been observed to occur for a single active column.

5.2 After-activity

If a complete assembly (a full pattern) is stimulated, a peak of activity occurs, fig. 3 (upper). The activity is terminated due to the adaptation of the cells. When the application of a neuromodulator like serotonin is simulated by decreasing the conductance of the Ca-dependent K-channel (see (Fransén *et al.* 1993), (Fransén and Lansner 1995b) and references therein) the activity in an activated assembly may instead persist, fig. 3 (lower). The after-activity is the result of a reduced adaptation of the cells due to a decreased conductance of the Ca-dependent K-channel which, in turn, is caused by the simulated neuromodulator application. The amount of modulator application will be given as a value between 0–100%, were 0% means no modulator, *i.e.* full adaptation, and 100% means no adaptation, *i.e.* no Ca-dependent K-channel conductance. With modulator application all stored patterns showed stable after-activity for 400–500 ms. This shows that the stored memories can be reliably recalled.

If the network is studied without simulated modulator application, the activity peak following the stimulation of a pattern will be followed by more peaks of activity from other patterns activated in succession. The different patterns that have been stored will in this way be activated in a non-trivial order due to their overlap. This feature is similar to that found in studies with reduced spiking models (Cartling 1995) and continuous output units (Cartling 1993). In that work this alternating activity pattern is named explorative in contrast to the case with modulator application which gives direct retrieval of one pattern.

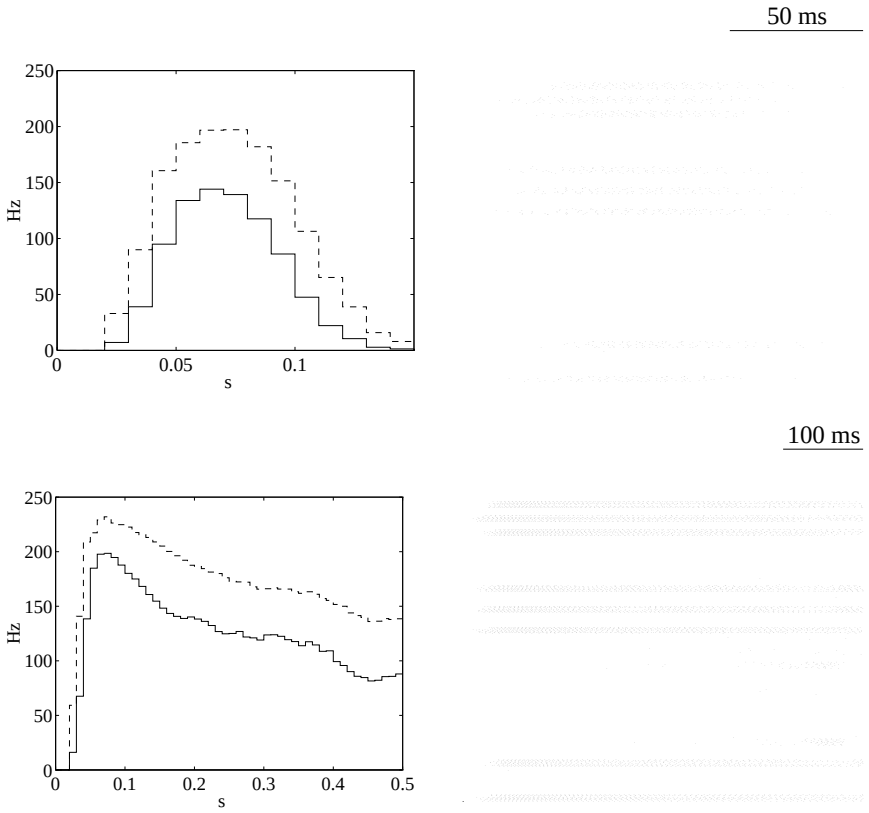

Figure 3: After-activity in one cell assembly. One full pattern is stimulated, first without simulated modulator application (upper), then with 60% modulator application (lower). In the first case only a transient activity peak occurs. In the second case spiking activity persists over 500 ms. Left: Mean spike rate histogram with standard deviation added on mean, and bin width 10 ms. Right: Spike raster plot showing all 600 pyramidal cells. The pattern is seen as 8 groups (columns no. 1, 6, 25, 28, 31, 39, 41, 43), each with 12 consecutive cells. The spurious activity that can be seen (especially around 360 ms) comes from columns that do not belong to any pattern and therefore lack (inhibitory) synaptic input. Simulated time 150 ms (upper) and 500 ms (lower) respectively. Stimulation with 0.2 nA for 50 ms on 8 of the 12 cells for each of the 8 columns in the pattern.

With the summing model commonly used for synapses, the frequency in the after-activity period would have been 150–200 Hz. Here, the firing rate is 70–100 Hz which is lower than the maximal due to the saturating conductance of the synaptic model (Fransén and Lansner 1995b). The small size of the assembly is one limiting factor when looking at low rates. With a larger assembly the rate can be closer to the 20–60 Hz reported from *in vivo* recordings. In previous studies a 200 pyramidal cell assembly, for instance, showed stable activity at 70 Hz (Fransén and Lansner 1995b).

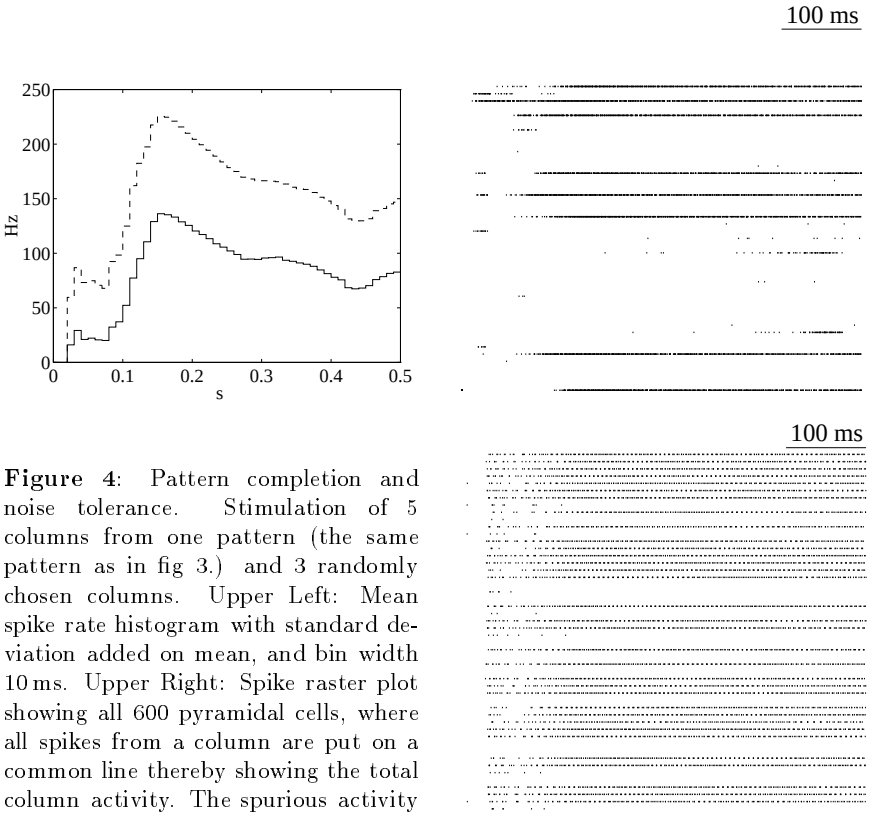

Figure 4: Pattern completion and noise tolerance. Stimulation of 5 columns from one pattern (the same pattern as in fig 3.) and 3 randomly chosen columns. Upper Left: Mean spike rate histogram with standard deviation added on mean, and bin width 10 ms. Upper Right: Spike raster plot showing all 600 pyramidal cells, where all spikes from a column are put on a common line thereby showing the total column activity. The spurious activity that can be seen in the right half of the plot comes, as in figure 3, from columns that do not belong to any pattern. Simulated time 500 ms with 60% modulator application. Stimulation with 0.2 nA for 50 ms on 8 of the 12 cells in a column. Lower Right: Spike raster plot showing all 150 inhibitory cells where all spikes from a column are put on a common line. Inhibitory inactive columns are either part of the active pattern or not part of any pattern.

5.3 Pattern Completion

When, for instance, 5 of the 8 columns in one assembly are stimulated the remaining 3 will get activated (pattern completion) by the inter-columnar excitatory connections. A few randomly activated columns added to the 5 stimulated columns will be suppressed (noise tolerance) as in fig. 4 (upper). All patterns were tested with a stimulation of 5 columns and they all completed their missing members and gave afteractivity for 400–500 ms. With less number of columns stimulated completion may get slower and less reliable. With just one or two stimulated columns the recalled pattern (if any) is not well defined. The inhibitory cell activity is essentially the complement of the excitatory on the column level, see fig. 4 (lower). This is analogous to findings in prefrontal cortex as discussed in the introduction.

The pattern completion and noise suppression are taking place shortly after stimulation has begun. This process is relatively fast, a complete pattern is normally obtained in 30–60 ms. It may thus be done within the initial activity peak without after-activity. This short reaction time can be compared to that found in psychophysical reaction time experiments (Thorpe and Imbert 1989), as has been discussed in previous work (Lansner and Fransén 1992). Those experiments set a lower limit of 100 ms for the identification of familiar visual objects.

5.4 Pattern Rivalry

An overlap between assemblies is essential for having an acceptable storage capacity. Despite this, an activated assembly will not produce any spurious secondary activation of columns in other assemblies. The spread of activation is prohibited by the lateral inhibition between assemblies. This pattern separation capability is also essential for a storage system. If the overlap is too large the assemblies can not be separated but will be grouped (activated) together. In our network the overlap between the 8 patterns with 8 columns each is 0–3. When parts of two assemblies are stimulated (conflicting input) they will compete. When one of the assemblies wins it will complete its pattern and shut down the activity in the other one, see fig. 5 (upper). This would be the physiological correlate of perceptual rivalry effects. Note in the figure (fig. 5 upper) that the firing pattern of individual cells varies considerably from rather regular to irregular (bursting). After-activity may here give the network more time to settle down in a stable complete activity pattern.

6 Scaling of Cell Numbers and Synaptic Distributions

The network we have simulated is very small which has forced us to compromises. In the first part of this section we will look at numbers and distributions of cells and synapses in the network and relate them to experimental findings. It is also important to show that the network performance does not degrade when numbers are increased and relative proportions of connections are changed towards more realistic values. In the latter part of this section we will study a scaling model and give an example using this.

In total our basic 50 column network has 12852 excitatory synapses and 1200 inhibitory synapses. In cortex the basket cell gives some 8 synapses on a target pyramidal cell (Martin 1988). This gives a multiplicative factor of 8 for the inhibitory synapses in the model when their number is compared to the excitatory synapses. For the basic model this yields 43% inhibitory synapses. This can be compared to the estimates of 11% reported for

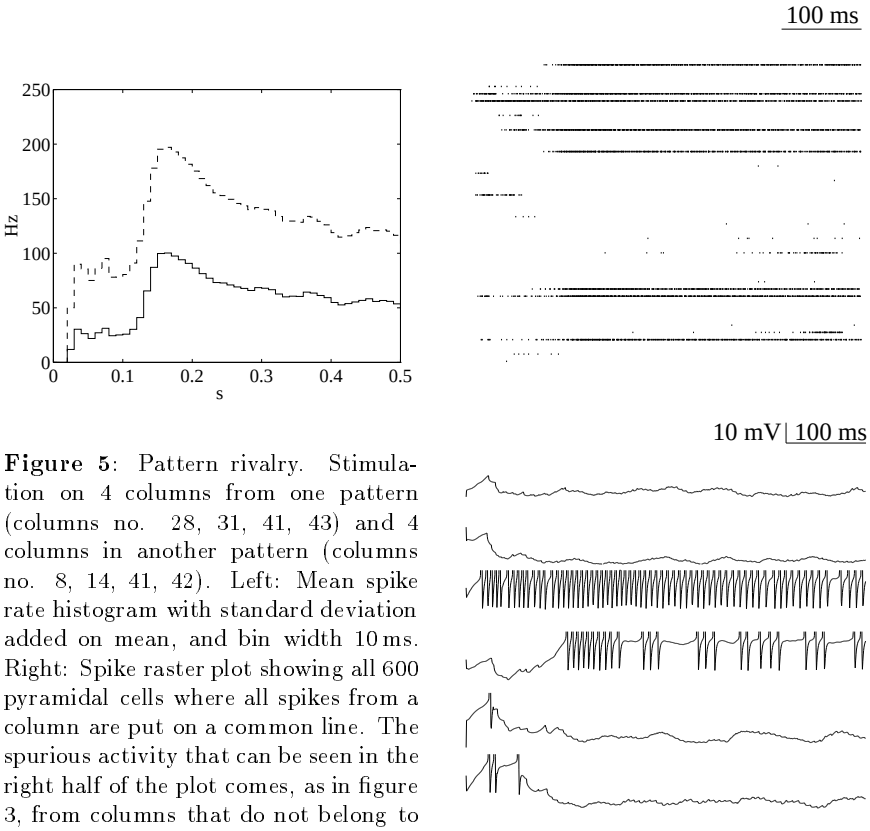

Figure 5: Pattern rivalry. Stimulation on 4 columns from one pattern (columns no. 28, 31, 41, 43) and 4 columns in another pattern (columns no. 8, 14, 41, 42). Left: Mean spike rate histogram with standard deviation added on mean, and bin width 10 ms. Right: Spike raster plot showing all 600 pyramidal cells where all spikes from a column are put on a common line. The spurious activity that can be seen in the right half of the plot comes, as in figure 3, from columns that do not belong to any pattern. Simulated time 500 ms with 60% modulator application. Stimulation with 0.2 nA for 50 ms on 8 of the 12 cells in a column. Lower Right: Pattern rivalry. Sample soma membrane potential for two cells in the winning pattern (middle two), two cells in the defeated pattern (lower two) and two cells of columns belonging to neither pattern (upper two). Action potentials are truncated.

inhibitory synapses (Schüz and Palm 1989). Our relatively large number of inhibitory synapses was a consequence of the requirement of a sufficient number of IPSP:s per unit time on an inhibited cell. For a somewhat larger simulated network of 169 columns trained with 21 patterns with 14 columns per pattern, the proportion was 21%. In the scaling example below we could adhere to the experimental value.

Concerning the density of connections, about half of the pyramidal cells have been estimated to send out lateral connections (Cynader and co-workers 1988). This figure is used in our scaling model and roughly realized in our basic model. Further, we have assumed that they all send local connections. As the local volume is much smaller than the volume restricted by the lateral connections (extending up to some 8 mm), local connectivity gets relatively dense and long-range very sparse. We shall return to this in

a paragraph below. In cortex the proportion of inhibitory cells is only 20%, and furthermore the inhibitory cells have a much smaller membrane area. In our basic network the inhibitory cell has 15 times more input synapses compared to an excitatory cell. This number decreases when the network is scaled (as will be shown below), but the denser connectivity is in agreement with the observation that inhibitory cells have about one order of magnitude larger synaptic density than pyramidal cells (McGuire *et al.* 1991).

It has been reported that the local connection probability between pyramidal cells is in the order of 9% (Mason *et al.* 1991; Nicoll and Blakemore 1993). In the basic example the local synapses give a larger probability, 53%, because the number of cells per column is so small (see also the discussion on local and long-range connections below). Two cells are quite rarely mutually connected (Mason *et al.* 1991). In our 50 column network the probability of a reciprocally connected pair in a column is 28% and between columns it is 0.5%. The intracolumn probability is again high due to the small number of cells per column.

Generally, we have used a "functional" strategy when looking how to define the scaling equations. By this we mean for instance observing how the number of active synapses on a cell scales. In average in the basic example an RS-cell gets 5.8 synapses from its column neighbors and 2.9 synapses from RS-cells in the other 7 columns of an active pattern. As mentioned before, these numbers are small as the network only represents a sub-sampling. The relative proportion, however, is satisfactory as it allows a cell to be activated by local as well as distant inputs.

Regarding the origin of synapses, 72% has been estimated to be local connections within a radius of $300\mu m$ and 28% outside (Nicoll and Blakemore 1993). For smaller radii, like the one of our columns, the proportion of local connections is most likely smaller. If we assume that there is a Gaussian connection probability we get 1.3% inside our column, which will be used in the scaling model. For the basic 50 column network we have 29% intracolumnar connections as too few local synapses per cell otherwise would prevent the cells within the column to be enough correlated.

As for the number of cells in a column, the number of neurons underneath a square millimeter cortex has been estimated to be 146,000 (Rockel *et al.* 1980) (except for primary visual cortex where it is about 2.5 times greater). A column is here estimated to be $50 \times 50\mu$m. This estimate is taken from the 800–1000μm found for the distance between ocular dominance columns (Löwel 1994), each housing some 18 iso-orientation columns, and the distance of 56μm between clusters of apical dendrites (Peters and Yilmaz 1993). Based on the number of neurons per square millimeter and the size of a column, the number of neurons in an orientation column can be estimated to some 900. Other areas than V1 thus would have some 350 neurons if the same area is assumed. As the lamina II/III cells constitute some third of these (Peters and Yilmaz 1993) we will below use 120 cells as

our estimate of the number of lamina II/III RS-cells and 30 for the FS-cells.

Quantity	*50 columns*	*169 columns*	*scaling ex.*	*cortex*
percent inhibitory synapses	43	21	11	11
percent local connections	29	11	1.3	72 (1.3*)
local connection probability	0.53	0.53	0.16	0.09

Table 1: Summary of relative proportions. * Our estimate.

To study how the network might be scaled up towards more realistic sizes, we have set up a number of scaling equations for different quantities. The equations are found in appendix B and their predictions will here be visualized by an example. As a starting point we take the upper 8 mm length of a long-range connection that has been reported. We use this length as the diagonal in a square piece of cortex which then gets a side of 5.7 mm. For this area we get 12800 columns of side 50μm. For the proportion of local synapses we take our estimate of 1.3% and for the proportion of inhibitory synapses we take the 11% that was experimentally reported. From the discussion of cell numbers above we will assume we have 120 RS-cells and 30 FS-cells per column. The increased size of the column will have a beneficial effect, an increased number of cells per pattern will also give decreased firing rates (Fransén and Lansner 1995b). Further, we will assume an average activity level of 1% of the cells which gives us a pattern size of 128. As an estimate of the number of active long-range synapses onto a cell in a pattern we have chosen 10, based on previous experiences with the 50 column network. This is probably at the lower end, but one should also remember that this network is only a part of the whole network and thus can not account for all the synaptic connectivity. As this value is three times that for the 50 column network, the PSP:s could here be correspondingly smaller. A detailed account of the calculations can be found in appendix B and a summary of some of the numbers in table 1.

Assuming theses values we get 1.55 billion long-range synapses to RS-cells and 0.39 billion long-range synapses on the FS-cells. The former value gives some 1008 synapses per receiving RS-cell. From the latter number we get 1027 synapses per receiving FS-cell and 257 synapses per sending RS-cell. These numbers are still a bit small but become adequate if larger patches are considered. Also, this is as already mentioned only a part of the cortical network. We have for instance not included the afference from lamina IV and other vertical circuitry. The 2530 synapses we get for a sending cell is quite reasonable. For the local connection probability our derived value of 0.16 is only a factor 2 off which is quite satisfactory. The value for the number of (local) synapses per FS-cell gives some 2850 synapses on the 120 RS-cells which should be enough to control the column activity. Finally, the value for the number of local synapses per RS-cell gives 19 synapses per cell. The number of active long-range synapses per cell was set to 10 so both types should have about equal possibility of affecting the cell.

7 Discussion

In our model we have obviously done several simplifications. For instance, the cortex has six lamina with recurrent connections between them. We have assumed that, except for the input from lamina IV, the influence in lamina II/III from the vertical connections is weak for the memory functions studied. Given this, the lamina II/III, together with its horizontal connections and input from lamina IV, may be studied separately.

It is not shown experimentally that interconnected areas are fully and functionally symmetrically connected. The instances examined experimentally where two cells have mutual connections indicate that the synaptic efficacies are not of equal size (Mason *et al.* 1991), *i.e.* there is asymmetric connectivity at the cell level. It is however not known what circuit these synapses belong to. A network supporting sequential association, for instance, would be expected to have an asymmetric connectivity. Further, the total effect of one column on another has not been determined experimentally to our knowledge.

The purpose of the scaling example was to show how our 50 column network might be scaled up towards more realistic sizes. The scaling model also produces some values that can be compared to those experimentally found. The network does not need to be limited to the 5.7×5.7 mm given in the example. A sub-sampling of columns over a larger area, where the inter-column fibers are myelinated, would be equivalent. The scaling model does not allow for an arbitrarily large number of columns, as discussed in appendix B. For large numbers, additional factors such as sparsity in the connectivity between columns would have to be included. A larger pattern can possibly tolerate not to be all-to-all even between columns, and still function as an entity. Also, when the number of columns per pattern increases one may get increased robustness for pattern completion (this was noted for the 169 column example).

For the 50 column network, the pattern size of 8 is somewhat smaller than the 11 proposed by the theoretical optimum. The size was chosen smaller as it was believed to better suit this small 50 column network. In the scaling example the pattern size of 1% is a factor 5 higher than the optimum (Lansner and Ekeberg 1985), and will give better redundancy at a price of lower storage capacity. For the selected activity level we will thus have 1% activity among the RS-cells. We also get activity in most FS-cells of columns which are correlated with but do not belong to the active pattern, yielding a much higher activity level among this class of inhibitory neurons.

A key feature of this model is the assumption that a cortical column is the basic computational unit. A possible explanation, suggested by our model, for the existence of functionally similar cells in cortical columns is that this duplication of cells is necessary in order to support a large enough

number of connections to other parts of the cortex. Hebb suggested that the cell assembly was the basic representational unit. This gives a distributed representation which can possibly extend over large cortical regions. With a low activity level as discussed above, such an entity will be difficult to detect experimentally. One further explanation why assemblies have not been found so far can be taken from the suggestions made by Cynader and co-workers (1988) that computational maps representing "information-bearing parameters" need to have little or no topographic order.

In this work a top-down strategy was used. We started with the connectivity of a recurrent ANN and looked at the features of a more biologically feasible model. Despite the simplifications and approximate nature of this model, we find it encouraging that a relatively biological model, can be derived in this way. As the basic connectivity comes from an ANN, the computational features of the model may be efficiently studied and evaluated. This strategy is now continued in a study of a higher order network with hyper columns (Lansner *et al.* 1996).

8 Conclusions

Attractor network models of cortical associative memory functions have developed considerably over the past few years. Here we show that we can improve them further, in terms of correspondence with cortical connectivity, by using multiple cells in lamina II/III of cortical columns connected by long-range fibers as the functional unit in the network instead of just a single cell. The connectivity of the model then becomes more realistic, since the original dense and symmetric connectivity now may be sparse and strongly asymmetric at the cell-to-cell level. Our simulations show that this kind of network, with model neurons of the Hodgkin-Huxley type arranged in columns, can operate as an associative memory in much the same way as previous models having a simpler connectivity. Cell activities comply with experimental findings and reaction times are within biological and psychological ranges. By introducing a scaling model we make it plausible that a network approaching experimentally reported neuron numbers and synaptic distributions also could work like the network studied here.

9 Acknowledgments

We would like to thank Mikael Djurfeldt, Örjan Ekeberg, Anders Holst and Jesper Tegnér for valuable discussions and comments, and Örjan Ekeberg and Per Hammarlund for supplying excellent simulation software. This work was supported by the Swedish Natural Science Research Council, grant no F–FU 06445–307.

References

Amit D J, Evans M R, Abeles M (1990) Attractor neural networks with biological probe records. *Network* **1**: 381–405.

Baranyi A, Szente M B, Woody C D (1993) Electrophysiological characterisation of different types of neurons recorded in vivo in the motor cortex of the cat. II. membrane parameters, action potentials, current-induced voltage responses and electrotonic structures. *J. Neurophysiol.* **69**: 1865–1879.

Bernander Ö, Douglas R J, Martin K A C, Koch C (1991) Synaptic background activity influences spatiotemporal integration in single pyramidal cells. *Proc. Nat. Acad. Sci. USA* **88**: 11569–11573.

Blasdel G G, Lund J S, Fitzpatrick D (1985) Intrinsic connections of macaque striate cortex: Axonal projections of cells outside lamina 4C. *J. Neurosci.* **5**: 3350–3369.

Brodin L, Tråvén H, Lansner A, Wallén P, Ekeberg Ö, Grillner S (1991) Computer simulations of N-methyl-D-aspartate (NMDA) receptor induced membrane properties in a neuron model. *J. Neurophysiol.* **66**: 473–484.

Buhl E H, Halasy K, Somogyi P (1994) Diverse sources of hippocampal unitary inhibitory postsynaptic potentials and the number of synaptic release sites. *Nature* **368**: 823–828.

Cartling B (1993) Control of the complexity of associative memory dynamics by neuronal adaptation. *Int. J. Neural Systems* **4**: 129–141.

Cartling B (1995) Autonomous neuromodulatory control of associative processes. *Network* **6**: 247–260.

Cavada C, Goldman-Rakic P (1989) Posterior parietal cortex in rhesus monkey: Evidence for segregated corticocortical networks linking sensory and limbic areas with the frontal lobe. *J. Comp. Neurol.* **287**: 422–445.

Connors B W, Gutnick M J (1990) Intrinsic firing patterns of diverse neocortical neurons. *TINS* **13**: 99–104.

Connors B W, Gutnick M J, Prince D A (1982) Electrophysiological properties of neocortical neurons in vitro. *J. Neurophysiol.* **48**: 1302–1320.

Cynader M S, co-workers (1988) General principles of cortical operation. In: Rakic P, Singer W, eds. Neurobiology of Neocortex. John Wiley New York. pp. 353–371.

Douglas R J, Martin K A C, Whitteridge D (1991) An intracellular analysis of the visual responses of neurones in cat visual cortex. *J. Physiol.* **440**: 659–696.

Ekeberg Ö, Hammarlund P, Levin B, Lansner A (1994) SWIM — A simulation environment for realistic neural network modeling. In: Skrzypek J, ed. Neural Network Simulation Environments. Kluwer Hingham, MA.

Ekeberg Ö, Wallén P, Lansner A, Tråvén H, Brodin L, Grillner S (1991) A computer based model for realistic simulations of neural networks. I: The single neuron and synaptic interaction. *Biol. Cybern.* **65**:81–90.

Ferster D, Lindström S (1983) An intracellular analysis of geniculo-cortical connectivity in area 17 of the cat. *J. Physiol.* **342**:181–215.

Ferster D, Lindström S (1985) Synaptic excitation of neurons in area 17 of the cat by intracortical axon collaterals of cortico-geniculate cells. *J. Physiol.* **367**:233–252.

Foehring R C, Lorenzon N M, Herron P, Wilson C J (1991) Corelation of physiologically and morphologically identified neuronal types in human association cortex in vitro. *J. Neurophysiol.* **66**:1825–1837.

Fransén E, Lansner A (1995a) Low spiking rates in a network with overlapping assemblies. In: Bower J M, ed. The Neurobiology of Computation: Proceedings of the Annual Computational Neuroscience Meeting. Kluwer Boston, MA, pp. 203–208.

Fransén E, Lansner A (1995b) Low spiking rates in a population of mutually exciting pyramidal cells. *Network* **6**:271–288.

Fransén E, Lansner A, Liljenström H (1993) A model of cortical associative memory based on Hebbian cell assemblies. In: Eeckman F H, Bower J M, eds. Computation and Neural Systems. Kluwer Boston, MA, pp. 431–435.

Funahashi S, Bruce C J, Goldman-Rakic P S (1989) Mnemonic coding of visual space in the monkey's dorsolateral prefrontal cortex. *J. Neurophysiol.* **61**:331–349.

Fuster J M, Jervey J P (1982) Neuronal firing in the inferotemporal cortex of the monkey in a visual memory task. *J. Neurosci.* **2**:361–375.

Gilbert C D, Hirsch J A, Wiesel T N (1990) Lateral interactions in visual cortex. In: Cold Spring Harbor Symposia on Quantitative Biology, volume LV. Cold Spring Harbor Laboratory Press. pp. 663–676.

Gilbert C D, Kelly J P (1975) The projections of cells in different layers of the cat's visual cortex. *J. Comp. Neurol.* **163**:81–106.

Gilbert C D, Wiesel T N (1979) Morphology and intracortical projections of functionally characterised neurones in the cat visual cortex. *Nature* **280**:120–125.

Goldman-Rakic P S (1988) Topography of cognition: Parallel distributed networks in primate association cortex. *Ann. Rev. Neurosci.* **11**:137–156.

Goldman-Rakic P S (1995) Cellular basis of working memory. *Neuron* **14**:477–485.

Hammarlund P, Ekeberg Ö (1996). Large neural network simulations on multiple hardware platforms. (In preparation.).

Hata Y, Tsumoto T, Sato H, Hagihara K, Tamura H (1993) Development of local horizontal interactions in cat visual cortex studied by cross-correlation analysis. *J. Neurophysiol.* **69**:40–56.

Hevner R F (1993) More modules. *Trends Neurosci.* **16**:178.

Hevner R F, Wong-Riley M T T (1992) Entorhinal cortex of the human, monkey, and rat: Metabolic map as revealed by cytochrome oxidase. *J. Comp. Neurol.* **326**:451–469.

Hirsch J A, Gilbert C D (1991) Synaptic physiology of horizontal connections in the cat's visual cortex. *J. Neurosci.* **11**:1800–1809.

Hopfield J (1982) Neural networks and physical systems with emergent collective computational abilities. *Proc. Natl. Acad. Sci. USA* **79**:2554–2558.

Hubel D H, Wiesel T N (1962) Receptive fields, binocular interaction and functional architecture in the cat's visual cortex. *J. Physiol.* **160**:106–154.

Katz L C, Callaway E M (1992) Development of local circuits in mammalian visual cortex. *Ann. Rev. Neurosci.* **15**:31–56.

Kawaguchi Y (1995) Physiological subgroups of nonpyramidal cells with specific morphological characteristics in layer II/III of rat frontal cortex. *J. Neurosci.* **15**:2638–2655.

Kisvarday Z F, Cowey A, Smith A D, Somogyi P (1989) Interlaminar and lateral excitatory amino acid connections in the striate cortex of monkey. *J. Neurosci.* **9**:667–682.

Lacaille J C (1991) Postsynaptic potentials mediated by excitatory and inhibitory amino acids in interneurons of stratum pyramidale of the CA1 region of rat hippocampal slices in vitro. *J. Neurophysiol.* **66**:1441–1454.

Lansner A, Ekeberg Ö (1985) Reliability and speed of recall in an associative network. *IEEE Trans. Pat. Analysis and Mach. Intelligence* **7**:490–498.

Lansner A, Ekeberg Ö (1989) A one-layer feedback, artificial neural network with a Bayesian learning rule. *Int. J. Neural Systems* **1**:77–87.

Lansner A, Ekeberg Ö, Fransén E, Hammarlund P, Wilhelmsson T (1996). Detailed simulation of large scale neural network models. (Submitted to CNS*96).

Lansner A, Fransén E (1992) Modelling Hebbian cell assemblies comprised of cortical neurons. *Network* **3**:105–119.

Lansner A, Fransén E (1995) Improving the realism of attractor models by using cortical columns as functional units. In: Bower J M, ed. The Neurobiology of Computation: Proceedings of the Annual Computational Neuroscience Meeting. Kluwer Boston, MA, pp. 251–256.

Lansner A, Holst A (1996). A higher order Bayesian neural network with spiking units. (in press).

Löwel S (1994) Ocular dominance column development: Strabismus changes the spacing of adjacent columns in cat visual cortex. *J. Neurosci.* **14**:7451–7468.

Martin K A C (1988) From single cells to simple circuits in the cerebral cortex. *Quarterly J. of Exp. Physiol.* **73**:637–702.

Mason A, Nicoll A, Stratford K (1991) Synaptic transmission between individual pyramidal neurons of the rat visual cortex *in vitro*. *J. Neurosci.* **11**:72–84.

McCormick D A, Connors B W, Lighthall J W (1985) Comparative electrophysiology of pyramidal and sparsely spiny stellate neurons of the neocortex. *J. Neurophysiol.* **54**:782–806.

McGuire B A, Gilbert C D, Rivlin P K, Wiesel T N (1991) Targets of horizontal connections in macaque primary visual cortex. *J. Comp. Neurol.* **305**:370–392.

Miyashita Y (1988) Neuronal correlate of visual associative long-term memory in the primate temporal cortex. *Nature* **335**:817–820.

Miyashita Y, Chang H S (1988) Neuronal correlate of pictorial short-term memory in the primate temporal cortex. *Nature* **331**:68–70.

Mountcastle V B (1957) Modality and topographic properties of single neurons of cat's somatic sensory cortex. *J. Neurophysiol.* **20**:408–434.

Nicoll A, Blakemore C (1993) Patterns of local connectivity in the neocortex. *Neur. Comput.* **5**:665–680.

Nicoll R A (1994) Cajal's rational psychology. *Trends Neurosci.* **368**:808–809.

Peters A, Yilmaz E (1993) Neuronal organization in area 17 of cat visual cortex. *Cerebral Cortex* **3**:49–68.

Rockel A J, Hiorns R W, Powell T P S (1980) The basic uniformity in structure of the neocortex. *Brain* **103**:221–244.

Scholfield C N (1978) Electrical properties of neurons in the olfactory cortex in vitro. *J. Physiol.* **275**:535–546.

Schüz A, Palm G (1989) Density of neurons and synapses in the cerebral cortex of the mouse. *J. Comparative Neurology* **286**: 442–455.

Shepherd G M, Koch C (1990) Dendritic electrotonus and synaptic integration. In: Shepherd G M, ed. The Synaptic Organization of the Brain. Oxford University Press New York and Oxford. pp. 462.

Smolensky P (1986) Information processing in dynamical systems: Foundations of harmony theory. In: E. R D, McClelland J L, eds. Parallel Distributed Processing (vol. 1). The MIT Press. pp. 195–281.

Somogyi P, Cowey A, Kisvárday Z F, Freund T F, Szentágothai J (1983) Retrograde transport of $\gamma-amino[^3H]butyric$ acid reveals specific interlaminar connections in the striate cortex of monkey. *Proc. Nat. Acad. Sci. USA* **80**: 2385–2389.

Somogyi P, Martin K A C (1985) Cortical circuitry underlying inhibitory processes in cat area 17. In: Rose D, Dobson V G, eds. Models of the Visual Cortex. John Wiley New York. pp. 514–523.

Szentágothai J (1978) The neuron network of the cerebral cortex: a functional interpretation. *Proc. Roy. Soc. London B* **201**: 219–248.

Thomson A M, Deuchars J (1994) Temporal and spatial properties of local circuits in neocortex. *Trends Neurosci.* **17**: 119–126.

Thorpe S, Imbert M (1989) Biological constraints on connectionist modelling. In: Pfeifer R, ed. Connectionism in Perspective. Springer-Verlag Berlin.

Tråvén H, Brodin L, Lansner A, Ekeberg Ö, Wallén P, Grillner S (1993) Computer simulations of NMDA and non-NMDA receptor-mediated synaptic drive — sensory and supraspinal modulation of neurons and small networks. *J. Neurophysiol.* **70**: 695–709.

Ts'o D Y, Gilbert C D, Wiesel T N (1986) Relationship between horizontal interactions and functional architecture in cat striate cortex as revealed by cross-correlation analysis. *J. Neurosci.* **6**: 1160–1170.

Vogt B A (1985) Electrophysiological properties of cingulate neurons. In: Peters A, Jones E G, eds. Cerebral Cortex 4. Plenum Press New York and London. pp. 133–149.

Wallén P, Ekeberg Ö, Lansner A, Brodin L, Tråvén H, Grillner S (1992) A computer-based model for realistic simulations of neural networks. II: The segmental network generating locomotor rhythmicity in the lamprey. *J. Neurophysiol.* **68**: 1939–1950.

Weliky M, Katz L C (1994) Functional mapping of horizontal connections in developing ferret visual cortex: Experiments and modeling. *J. Neurosci.* **14**: 7291–7305.

Wilson F A W, Scalaidhe S P Ó, Goldman-Rakic P S (1994) Functional synergism between putative γ-aminobutyrate-containing neurons and pyramidal neurons in prefrontal cortex. *Proc. Nat. Acad. Sci. USA* **91**: 4009–4013.

Appendix A

The ANN model

The Bayesian neural network model (Lansner and Ekeberg 1989) is designed to calculate the posterior probabilities of some output attributes given some input attributes. In the network there is one unit for each input attribute x_i and each output attribute y_j. If Bayes rule for conditional probabilities is combined with an assumption of independent input attributes we get:

$$P(y \mid \boldsymbol{x}) = P(y)\frac{P(\boldsymbol{x} \mid y)}{P(\boldsymbol{x})} = P(y)\frac{P(x_1 \mid y)}{P(x_1)}\frac{P(x_2 \mid y)}{P(x_2)} \cdots \frac{P(x_n \mid y)}{P(x_n)} \qquad (1)$$

When taking the logarithm (base e) of (1) the right hand side becomes a sum. In this sum each term (except the first) corresponds to the weight w_{ji} from unit x_i to unit y_j:

$$w_{ji} = \log\left(\frac{P(x_i \mid y_j)}{P(x_i)}\right)$$

and the bias β_j can be identified as the first term:

$$\beta_j = \log(P(y_j)) \qquad (2)$$

Each output unit sums its inputs and exponentiates the result, yielding the desired probability. If the independence assumption is relaxed a higher order network results (Lansner and Holst 1996).

In the ANN used there is no difference between input and output units, so all units receive inputs from all others as well as external input. For the network the following also hold:
$m = k_m \log N, \quad k_m \approx 2.7$
$Z_m = k_z N^2/log^2 N, \quad k_z \approx 0.14$

We set the current for the à *priori* activity according to: $I_\beta = k_\beta e^{\beta_j}$
The current for a cell which is part of the pattern is set to: $I_+ = I_{stim}$
and a current for a cell which is not part of the pattern: $I_- = k_- e^{\beta_j}\alpha$
where k_β and k_- are scaling constants and $\alpha = 1/Z$

N number of columns
m number of columns per pattern
n number of pyramidal cells per column[1]
Z number of stored patterns
Z_m maximal number of patterns that can be stored

[1] The number of inhibitory cells is $0.25\ n$.

Appendix B

Scaling equations for the network

The following equations define the scaling model of which the 50 column network is the starting point. Notations are according to appendix A.

number of RS-RS synapses within the column:

$$s_{le} = k_e n, \quad k_e \leq n \tag{3}$$

number of FS-RS synapses within the column[2]:

$$s_{li} = k_i 0.25n, \quad k_i \leq 8n \tag{4}$$

number of RS-RS synapses between columns[3]:

$$s_{ge} = \frac{N^2 f_e}{2} \tag{5}$$

number of RS-FS synapses between columns[3]:

$$s_{gi} = \frac{N^2 f_i}{2} \tag{6}$$

proportion of excitatory synapses: (we use eq. 3, 5, 6)

$$p_e = \frac{N s_{le}}{N s_{le} + s_{ge} + s_{gi}} = \frac{1}{1 + \frac{N(f_e + f_i)}{2nk_e}} \tag{7}$$

$$\Rightarrow k_e = \frac{1.25 f_e}{\frac{2n}{N}(\frac{1}{p_e} - 1) - 0.25} \tag{8}$$

proportion of inhibitory synapses: (we use eq. 3, 4, 5, 6, 7)

$$p_i = \frac{8N s_{li}}{8N s_{li} + N s_{le} + s_{ge} + s_{gi}} = \frac{1}{1 + \frac{k_e}{2k_i p_e}} \tag{9}$$

$$\Rightarrow k_i = \frac{k_e}{2p_e(\frac{1}{p_i} - 1)} \tag{10}$$

number of active intercolumnar synapses per RS-cell:

$$s_a = \frac{m-1}{N}\frac{s_{ge}}{Nn} = \frac{(m-1)f_e}{2n} \tag{11}$$

$$\Rightarrow \quad f_e = \frac{2 s_a n}{m-1} \tag{12}$$

[2]In cortex 80% excitatory and 20% inhibitory neurons are reported by *i.e.* (Gilbert *et al.* 1990; Katz and Callaway 1992), and the basket cell is shown to give some 8 synapses on a target pyramidal cell (Martin 1988).

[3]For a reasonably well filled network the number of connections to columns, with RS-cells or FS-cells as targets, are equal and nonzero.

proportion of intercolumnar sending cells[4]:

$$o_e + o_i = 0.5n \qquad (13) \qquad \Rightarrow \quad o_i = 0.5n - o_e \qquad (14)$$

proportion of FS-cells that are connected by one RS-cell[5]:

$$\frac{Nf_i}{2} = 0.25(\frac{Nf_e}{2} + nk_e) \qquad (15) \qquad \Rightarrow \quad f_i = 0.25(f_e + \frac{2nk_e}{N}) \qquad (16)$$

total number of connections in s_{ge} and s_{gi}:

$$fo_e = \frac{N^2 f_e}{2N}, fo_i = \frac{N^2 f_i}{2N} \qquad (17) \qquad \Rightarrow \quad f = \frac{Nf_e}{2o_e} = \frac{Nf_i}{2o_i} \qquad (18)$$

the two expressions in 17 are equal:

$$\frac{o_e}{f_e} = \frac{o_i}{f_i} \qquad (19) \quad \text{use eq. 14, 16} \quad \Rightarrow \quad o_e = \frac{1}{\frac{2.5}{n} + \frac{k_e}{Nf_e}} \qquad (20)$$

connection probability between RS-cells in a column:

$$p_c = \frac{\frac{s_{1e}}{n}}{n-1} = \frac{k_e}{n-1} \qquad (21)$$

k_e number of synapses to and from an RS-cell
k_i number of synapses from an FS-cell
f_e number of synapses to RS-cells between two connected columns
f_i number of synapses to FS-cells between two connected columns
o_e number of RS-cells per column sending long-range synapses
o_i number of FS-cells per column sending long-range synapses
f number of synaptic terminals per RS-cell sending long-range synapses

As discussed in sect. 6 we assume $N = 12800$, $n = 120$, $m = 128$, $p_e = 0.013$, $p_i = 0.11$ and $s_a = 10$. From this we get $f_e = 19$ using eq. 12. From f_e we get $s_{ge} = 1.55 \cdot 10^9$ by using eq. 5 and $k_e = 19$ by using eq. 8. From k_e we get $k_i = 95$ using eq. 10, $f_i = 4.8$ using eq. 16, $o_e = 48$ using eq. 20, and $p_c = 0.16$ from eq. 21. With f_i in turn we get $s_{gi} = 0.39 \cdot 10^9$ from eq. 6. Last, with o_e we get $f = 2530$ from eq. 18 and $o_i = 12$ from eq. 14. a Our scaling equations do not allow for arbitrary large number of columns N. The major problem is the quadratic dependence on N for s_{ge} and s_{gi}. For larger spatial distances in cortex it is reasonable to assume that the number of connections grow with something in between N and N^2. By introducing a constant multiplicative factor less than 1 to s_{ge}

[4]Roughly half of the pyramidal cells have been estimated to send out lateral connections (Cynader and co-workers 1988).

[5]Pyramidal cells are reported to have 81% pyramidal cells and 19% inhibitory cells as targets (McGuire *et al.* 1991).

and s_{gi}, much larger N may be possible. In a preliminary study we have tested our ANN up to $N = 12800$ for different degrees of dilution. For the largest dilution where only 4% of the possible connections were present, the network could still store and reliably recall 1.4% of the maximal 256,000 patterns a full networks can store. For increasing N this fraction of stored patterns increased favorably with 0.4% per doubling of N.

Appendix C

Model Parameters

		Na^+		K^+	Ca^{2+}	NMDA
		m	h	n	q	p
α	A ($\mathrm{mV^{-1}\,ms^{-1}}$)	0.58	0.232	0.058	0.232	2.03 ($\mathrm{ms^{-1}}$)
	B (mV)	-50	-50	-50	10	–
	C (mV)	1	1	0.8	11	17
β	A ($\mathrm{mV^{-1}\,ms^{-1}}$)	0.174	1.16 ($\mathrm{ms^{-1}}$)	0.0145	0.0029	0.0292 ($\mathrm{ms^{-1}}$)
	B (mV)	-59	-46	-40	10	–
	C (mV)	20	2	0.4	0.5	17

Table 2: Parameters describing the ion channel kinetics.

Notes to table 2
Notations correspond to those used in (Ekeberg *et al.* 1991). Parameters values are according to (Fransén and Lansner 1995b).

*Parameter**	*Value FS*†	*Value RS*‡	*Note*	*Unit*	*Description*
E_{leak}	−75			mV	leak current equilibrium potential
E_{Na}	50			mV	sodium current equilibrium potential
E_K	−80			mV	potassium current equilibrium potential
E_{Ca}	150			mV	calcium current equilibrium potential (voltage gated)
$E_{Ca(NMDA)}$	20			mV	calcium current equilibrium potential (NMDA gated)
g_m	0.74	0.44	b	$\mu S mm^{-2}$	membrane leak conductance
C_m	0.01			$\mu F mm^{-2}$	membrane capacitance
g_{ext}	0.19	0.068	c	$\mu S mm^{-2}$	conductance from diffuse transmitter stimulation
Soma					parameters specific for the soma compartment
g_{Na}	150			$\mu S mm^{-2}$	sodium conductance
g_K	1002	84	d	$\mu S mm^{-2}$	potassium conductance
$g_{K(Ca)}(AHP)$	0.368×M	36.8×M	e	nS	potassium conductance (Ca^{2+} gated)
ρ_{AP}	1.0			$mV^{-1}ms^{-1}mm^{-2}$	Ca^{2+} inflow rate (voltage gated)
δ_{AP}	9			s^{-1}	Ca^{2+} decay rate (voltage entered Ca^{2+})
a_s	0.000154	0.00139	f	mm^2	soma membrane mean area
Initial segment					parameters specific for the initial segment
g_{Na}	2505			$\mu S mm^{-2}$	sodium conductance
g_K	5010	418	d	$\mu S mm^{-2}$	potassium conductance
g_{core}	300			$\mu S mm^{-2}$	core conductance per membrane area
a_{IS}	0.1			–	initial segment membrane area factor (fraction of soma area)
Dendrite					parameters specific for the dendrite compartments
$g_{K(Ca)}(NMDA)$	–	40×M	g	nS	potassium conductance (NMDA-Ca^{2+} gated)
δ_{NMDA}	–	2	g	s^{-1}	Ca^{2+} decay rate (NMDA entered Ca^{2+})
g_{core}	13.7	8.1	h	$\mu S mm^{-2}$	core conductance per membrane area
a_d	4			–	dendrite membrane area factor (fraction of soma area)

Table 3: Parameters describing the cell.

Notes to table 3
Here, M is the modulator multiplication factor. *Notations correspond to those used in (Ekeberg *et al.* 1991). †Values are the same as in (Fransén and Lansner 1995b) unless followed by a reference. ‡All values are the same as in (Fransén and Lansner 1995b). Only values differing from FS are listed.

[b] The value of FS: g_m is calculated from the time constant reported in (Kawaguchi 1995).
[c] The value of FS: g_{ext} is adjusted to give an (*in vivo*) resting potential of -60 mV. This is 10 mV below the firing level (Baranyi *et al.* 1993) which is 25 mV above the resting potential of -75 mV (Foehring *et al.* 1991), see also the discussions in (Baranyi *et al.* 1993; Scholfield 1978; Connors *et al.* 1982; Bernander *et al.* 1991; Vogt 1985) on *in vitro* and *in vivo* differences.
[d] The value of FS: g_K has been adjusted to give a shorter spike fall time and narrower spike width (McCormick *et al.* 1985; Connors and Gutnick 1990; Baranyi *et al.* 1993; Foehring *et al.* 1991). (The value of g_{Na} is the same as for RS (McCormick *et al.* 1985; Connors and Gutnick 1990; Baranyi *et al.* 1993; Foehring *et al.* 1991).)
[e] The value of FS: $g_{K(Ca)}$(AHP) has been set to give a barely noticeable AHP (McCormick *et al.* 1985; Connors and Gutnick 1990; Lacaille 1991; Baranyi *et al.* 1993; Foehring *et al.* 1991).
[f] The value of FS: a_s soma area from (McCormick *et al.* 1985; Foehring *et al.* 1991).
[g] The value is the same as in (Tråvén *et al.* 1993).
[h] The value of FS: g_{core} is calculated from a length constant of 0.233 per compartment. This is the same as for the RS-cell. See also the discussion in (Shepherd and Koch 1990) p 462 on the ever shorter electrotonic lengths used in simulations.

*Parameter**	*Value†*	*Note*	*Unit*	*Description*
kainate/AMPA synapse				parameters specific for the kainate/AMPA synapse
compartment	basal (C), medial (L), somatic (I)	i,j	–	location on postsynaptic target
E_{Na+K}	0		mV	equilibrium potential for Na^+/K^+ current
g_{exc}	0.38 (C), 1.4 (L), 0.072 (I)	k	nS	conductance after spike
t_{delay}	1		ms	time delay
$t_{duration}$	0		ms	open time
ρ_{syn}	0		ms	raise time constant
δ_{syn}	10		ms	closing (decay) time constant
$GABA_A$ synapse				parameters specific for the $GABA_A$ synapse
compartment	*soma*	l	–	location on postsynaptic target
E_{Cl}	−85	m	mV	equilibrium potential for Cl^- current
g_{inh}	10.0	k	nS	conductance after spike
t_{delay}	1	m	ms	time delay
$t_{duration}$	0	m	ms	open time
ρ_{syn}	0	m	ms	raise time constant
δ_{syn}	17	m	ms	closing (decay) time constant
NMDA synapse				parameters specific for the NMDA synapse
compartment	basal (C), medial (L)	i	–	location on postsynaptic target
E_{NMDA}	0		mV	equilibrium potential for Na^+/K^+ current
$E_{Ca(NMDA)}$	20		mV	equilibrium potential for Ca^{2+} current
g_{NMDA}	2.7 (C), 9.6 (L)	k	nS	conductance after spike
ρ_{NMDA}	$1.1 g_{NMDA}$	m	$s^{-1}mV^{-1}\mu S^{-1}$	Ca^{2+} inflow rate (NMDA gated)
t_{delay}	5		ms	time delay
$t_{duration}$	20		ms	open time
ρ_{syn}	5		ms	raise time constant
δ_{syn}	150		ms	closing (decay) time constant
noise synapse				parameters specific for the noise synapse
compartment	*proximal*		–	location on cell
E_{noise}	0		mV	equilibrium potential for noise synapse
g_{noise}	105 (RS), 23 (FS)	n	$pSmm^{-2}$	conductance of noise synapse
δ_{syn}	10		ms	closing (decay) time constant

Table 4: Parameters describing the synapse.

Notes to table 4
Notations correspond to those used in (Tråvén *et al.* 1993). †Values are the same as in (Fransén and Lansner 1995b) unless followed by a reference. (C) connection within the column, (L) long-range connection between columns, and (I) connection to a FS-cell.

[i] The combined kainate/AMPA and NMDA synaptic connection between RS-cells has been placed on the basal (local within column) (Nicoll and Blakemore 1993) or medial (long-range between columns) (McGuire *et al.* 1991) dendritic compartment.
[j] The synaptic connection between RS-cell and a FS-cell is a kainate/AMPA synapse. It has been placed on the soma compartment (Thomson and Deuchars 1994).
[k] The standard deviation of the conductance of each synaptic type is 20 % of its mean value. The synaptic conductances of the long-range RS-RS and RS-FS synapses come from a learning rule. The value refers to the average.
[l] The placement is somatic or proximal (Nicoll 1994; Buhl *et al.* 1994).
[m] The value is the same as in (Tråvén *et al.* 1993).
[n] The value of FS: g_{noise}, the conductance of the noise, is tuned to give some 1–3 spikes per 10 s as in (Fransén and Lansner 1995b). As described in (Wallén *et al.* 1992) the source of the synaptic noise is a Poisson process with an expectation value of 300 PSP:s per second.